Journal of Optometry 16 (2023) 53—63

Journal of Optometry

www.journalofoptometry.org

ORIGINAL ARTICLE

The effect of intrinsically photosensitive retinal ganglion cell (ipRGC) stimulation on axial length changes to imposed optical defocus in young adults

Ranjay Chakraborty[a,b,*], Michael J. Collins[c], Henry Kricancic[c], Brett Davis[c], David Alonso-Caneiro[c], Fan Yi[c], Karthikeyan Baskaran[d]

[a] *Caring Futures Institute, Flinders University, Bedford Park, SA 5042, Australia*
[b] *College of Nursing and Health Sciences, Optometry and Vision Science, Sturt North, Flinders University, Bedford Park, SA 5042, Australia*
[c] *Contact Lens and Visual Optics Laboratory, School of Optometry and Vision Science, Queensland University of Technology, Victoria Park Road, Kelvin Grove 4059, Brisbane, QLD, Australia*
[d] *Department of Medicine and Optometry, Linnaeus University, Kalmar, Sweden*

KEYWORDS
Intrinsically photosensitive retinal ganglion cells;
Axial length;
Melanopsin;
Optical defocus;
Myopia

Abstract
Purpose: The intrinsically photosensitive retinal ganglion cells (ipRGCs) regulate pupil size and circadian rhythms. Stimulation of the ipRGCs using short-wavelength blue light causes a sustained pupil constriction known as the post-illumination pupil response (PIPR). Here we examined the effects of ipRGC stimulation on axial length changes to imposed optical defocus in young adults.
Materials and methods: Nearly emmetropic young participants were given either myopic (+3 D, n = 16) or hyperopic (-3 D, n = 17) defocus in their right eye for 2 h. Before and after defocus, a series of axial length measurements for up to 180 s were performed in the right eye using the IOL Master following exposure to 5 s red (625 nm, 3.74×10^{14} photons/cm^2/s) and blue (470 nm, 3.29×10^{14} photons/cm^2/s) stimuli. The pupil measurements were collected from the left eye to track the ipRGC activity. The 6 s and 30 s PIPR, early and late area under the curve (AUC), and time to return to baseline were calculated.
Results: The PIPR with blue light was significantly stronger after 2 h of hyperopic defocus as indicated by a lower 6 and 30 s PIPR and a larger early and late AUC (all $p<0.05$). Short-wavelength ipRGC stimulation also significantly exaggerated the ocular response to hyperopic defocus, causing a significantly greater increase in axial length than that resulting from the hyperopic defocus alone (p = 0.017). Neither wavelength had any effect on axial length with myopic defocus.
Conclusions: These findings suggest an interaction between myopiagenic hyperopic defocus and ipRGC signaling.

* Corresponding author at: College of Nursing and Health Sciences, Optometry and Vision Science, Sturt North, Flinders University, Sturt Rd, Bedford Park, SA 5042, Australia.
E-mail address: ranjay.chakraborty@flinders.edu.au (R. Chakraborty).

https://doi.org/10.1016/j.optom.2022.04.002

Introduction

The intrinsically photosensitive retinal ganglion cells (ipRGCs) are a distinct subtype of ganglion cells that constitute only about 0.2 − 2.5% of all ganglion cells across species, with widespread dendritic coverage across the entire retina, except the fovea.[1-3] These cells contain a blue light sensitive photopigment, melanopsin, with a peak sensitivity at ~482 nm.[4,5] ipRGCs respond to light directly through melanopsin,[3] and indirectly through synaptically-mediated input from rod and cone photoreceptors.[6,7] The ipRGC axons project to several brain centers and regulate non-image forming functions, such as photoentrainment of circadian rhythms, regulation of pupillary light reflex (PLR), sleep, and alternes,[5,8-10] as well as contrast and color detection, and pattern vision.[11-13] It is unclear if melanopsin signaling influences refractive development of the eye.

The ipRGCs regulate visual functions either through their intrinsic light response or via synaptic connections with outer retinal photoreceptors and other retinal neurons (such as dopaminergic amacrine cells or DACs).[2,7,14] Studies have shown synaptic connections between DACs and ipRGCs in the inner plexiform layer of the retina[2,15] and evidence that these melanopsin cells may affect retinal dopamine release.[16,17] Alterations in retinal dopamine production and release may influence refractive development, as shown in animal models of myopia (see reviews).[18,19] In a recent study, the absence of the melanopsin photopigments in *Opn4*$^{-/-}$ mice resulted in abnormal refractive development and greater susceptibility to form-deprivation myopia.[20] The increased susceptibility to myopia in *Opn4*$^{-/-}$ mice was found to be associated with lower dopaminergic activity in the retina and was partly attenuated with L-DOPA treatment, suggesting that proper ipRGC function may be essential for normal refractive development, protection from myopia progression, and for maintaining intact retinal dopaminergic signaling.

In vivo ipRGC activity can be measured indirectly through the pupil response to short wavelength light.[4,21] Following short wavelength stimulation offset, the intrinsic response of ipRGCs produces a sustained pupil constriction, also known as the post-illumination pupil response (PIPR).[4,21-23] The PIPR redilation dynamics have been shown to correlate with the sustained firing pattern seen in single cell recordings,[4] and are a robust marker of ipRGC activity. Impaired ipRGC function and PIPR are associated with several ocular diseases.[24] Despite some evidence of a possible link between melanopsin function and refractive error development, previous studies,[22,25,26] including our own study,[27] found no significant association between refractive error and the ipRGC-driven PIPR in young adults and children.

It is noteworthy that these studies have all investigated the PIPR under 'natural' defocus state (i.e. with the actual refractive error) and not with 'imposed' defocus. Previous studies have shown that brief periods (1−2 h) of imposed defocus results in small, but significant changes in axial length (measured from the anterior corneal surface to the retinal pigment epithelium or RPE) and choroidal thickness of human subjects, which represents the effects of short-term optical blur to the eye.[28-30] Furthermore, visual processing of imposed optical defocus can be considerably different from natural defocus in human eyes.[31] The goal of this study was to examine the effects of melanopsin stimulation on axial length changes to imposed hyperopic and myopic defocus in young adult eyes to understand the interaction between melanopsin signaling and optical blur at the retina.

Materials and methods

Participants

Young adult participants between the ages of 18 and 25 years (mean ± SD, 21.67 ± 2.13) were recruited to examine the effects of melanopsin stimulation upon axial length changes to myopic (n = 16; male=7, female=9) and hyperopic (n = 17; male=8, female=9) defocus. 12 subjects participated in both defocus experiments. Prior to participation, all subjects underwent a comprehensive eye examination to assess their refractive status and ocular health. The mean spherical equivalent refraction (SER) was −0.26 ± 0.35 and −0.23 ± 0.31 DS for participants in myopic and hyperopic defocus experiments, respectively. All subjects had normal logMAR visual acuity of 0.00 or better, and astigmatic refractive error of ≤0.75 DC. No participants had ocular pathology or history of any major eye or refractive surgery.

None of the participants were taking any prescription medication known to affect the pupil size or sleep (such as melatonin). In addition, participants were asked to refrain from alcohol, caffeine and nicotine 12 h prior to the pupil measurements. All participants were tested between 9:00 am and 1:00 pm to minimize the effects of circadian variation on ipRGC function and the PIPR.[32] Approval from the Southern Adelaide Local Health Network (SALHN, ID: 156.17) was obtained, and all participants provided written informed consent prior to their participation. All subjects were treated in accordance with the Declaration of Helsinki.

The optical system for pupil measurements

The PIPR was measured using a custom-built optical system, as described previously[27] and shown in Fig. 1A and B and. The optical design was inspired by a previous publication by Kankipati et al.[23] Briefly, the illumination system consisted of a set of red and blue light-emitting diodes (LEDs). The light from the red and blue LEDs was transmitted to the right eye via two Fresnel lenses; F1 and F2, each of a 10.16 cm diameter and a 10.16 cm focal length (Edmund Optics, Barrington, NJ). The blue (470 nm, 3 mm diameter, full width at half maximum [FWHM] 22 nm) and red LEDs (625 nm, 3 mm diameter, FWHM 20 nm) (Jaycar Electronics, Rydalmere, Australia) were positioned at the focal length of the first Fresnel lens, F1. The two Fresnel lenses were kept 20.32 cm apart (i.e. separated by twice their focal length). A holographic diffuser of 5-degree diffusing angle (Edmund Optics, Barrington, NJ) was placed in front of the second Fresnel lens (F2), and the participant's right eye was positioned at the focal point of F2. During the PIPR measurement, the right eye was presented with the light stimulus, and the effect of light stimulation was measured in the contralateral

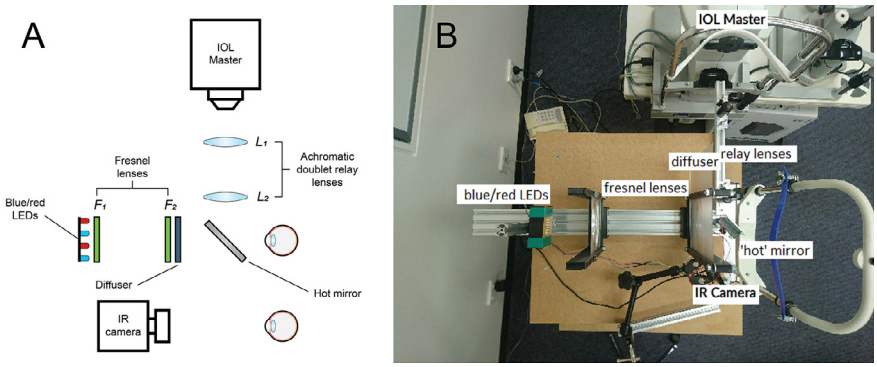

Fig. 1 Overview of the optical system used in the study; animated (A) and real image (B). Two fresnel lenses, F1 and F2 (both 10.16 cm focal length and diameter), were placed at twice their focal length apart. Red and blue LEDs were placed at one end of the optical system. The subject's right eye was aligned at the other end, while the left eye was recorded by the infrared camera (IR camera) attached to the computer. The diffuser had a 5 deg diffusing angle. The hot mirror and the two achromatic doublet relay lenses (L1 and L2, both 10 cm focal length) enabled axial length measurements using the IOL Master to be performed during red and blue light stimulation to the eye.

left eye using an infrared camera. A modified Logitech C920 HD Pro-webcam (Logitech, Newark, CA) with illuminating infrared LEDs (940 nm, 5 mm diameter, Core Electronics, NSW, Australia) was used to record the pupil responses from the left eye at a rate of 15 frames/s. The presentation of light stimulus and the duration of PIPR recording were controlled via a small single-board computer, Raspberry Pi 3 Model B (Core Electronics, NSW, Australia). During the experiment, the participants were positioned in a chinrest and instructed to look straight ahead at a small red laser spot on the wall at a 4 m distance to induce minimal accommodation.

For concurrent measurements of axial length and PIPR under natural binocular viewing conditions, a relay lens system, involving a 5 × 5 cm hot mirror and a pair of achromatic doublet lenses (L1 and L2) with focal lengths of 10 cm (Edmund Optics, Barrington, NJ), was used (Fig. 1). Briefly, the IOL Master 500 (Carl Zeiss, Jena, Germany) was kept at the focal point of the first lens L1 (close to 10 cm from L1). The two lenses L1 and L2 were separated by 20 cm to maintain the afocal optical system at 1x magnification.[33] Finally, the infrared measurement beam travelling from the IOL Master through the relay lens system was redirected towards the subject's right eye by a wide band hot mirror placed 5 cm in front of the subject's right eye at an angle of 45°. The optical system allowed the IOL Master's infrared beam (780 nm) as well as light from the red and blue LEDs to reach the right eye simultaneously, enabling the IOL Master measurements to be performed during red and blue light stimulation to the eye.

Pupillometry

The red and blue LEDs illuminating the eye were flickering at 10 Hz with a duty cycle of 80%. The corneal irradiance levels, measured using an optical power meter (Newport Corporation, Irvine, CA), were 3.29×10^{14} photons/cm^2/s for the blue stimulus (470 nm) and 3.74×10^{14} photons/cm^2/s for the red stimulus (625 nm). These corneal irradiances have previously been shown to induce a significant PIPR in young humans (27). The individual photoreceptor excitation (α-optic lux) with the red and blue light stimuli are shown in Table 1.[34]

In order to induce myopic and hyperopic defocus, participants wore a + 3.00 or −3.00 DS Proclear® 1 day daily disposable contact lens (CL, CooperVision, Pleasanton, CA) in their right eye for a period of two hours. For subjects with low refractive errors, the defocus was combined with the refractive correction into the CL power. Only emmetropic (or near emmetropic) participants were recruited so that participants can clearly view the distant target at 4 m from their uncorrected left eye and accurate pupil recordings can be captured from the left eye (without CL). The CL induced desired level of optical defocus in the right eye only, while the left eye had clear vision. On the day of the experiment, all participants reported to the laboratory between 9 - 9:30 am. Prior to any ocular measurement, participants were required to perform a binocular distance viewing task for 10 min (sitting and viewing an object at 6 m) in dim light of <10 lux to wash out any residual effects of previous visual tasks on measurements, as previously described.[35] Following the 10-minute wash out period, CLs were introduced, and the participants were dark adapted for 5 min. Immediately after dark adaptation, a series of axial length and PIPR measurements were performed in the defocused right eye over the CL (Fig. 2). More specifically, the right eye was

Table 1 Individual photoreceptor excitation (α-optic lux) with 470 nm 3.29×10^{14} photons/cm^2/s and 625 nm 3.74×10^{14} photons/cm^2/s light stimuli (based on Lucas et al.[34]).

		α-optic lux	
Photoreceptor class	Prefix	470 nm	625 nm
S cone	Cyanopic	952.98	0
Melanopsin	Melanopic	995.4	0.62
Rod	Rhodopic	684.3	4.49
M cone	Chloropic	329.1	88.93
L cone	Erythropic	162.83	334.11

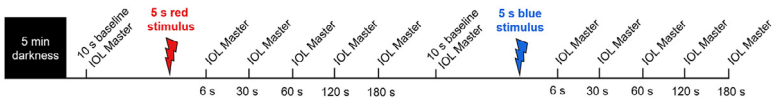

Fig. 2 Protocol for axial length measurements. Participants were given 5 min of dark adaptation before axial length and pupil measurements. Axial length measurements were obtained during 10 s pre-stimulus baseline period, and then 6 s, 30 s, 60 s, 120 s and 180 s after 5 s red stimulation. After another 10 s baseline, the same protocol was repeated for 5 s blue stimulation.

exposed to a 5 s pulse of red and blue light, and the consensual pupil responses were measured in the left eye for 100 s following light offset. The stimulus duration was chosen based on our previous study in which we found that a 5 s blue stimulus induced a much stronger melanopsin response compared to a 1 s stimulus of same wavelength.[27] For this experiment, the right eye was undilated to keep the magnitude of imposed defocus consistent throughout the experiment.

Following exposure to red and blue stimuli, a series of axial length measurements were obtained at baseline, and then at 6, 30, 60, 120 and 180 s after stimulus offset from the right eye, using the IOL Master 500 (Fig. 2). The IOL Master and pupil measurements were repeated after 2 h of exposure to defocus to examine the interaction between melanopsin stimulation and axial length changes to short-term optical blur. For this experiment, the PIPR measurements were collected until the pupil returned to baseline or end of the ipRGC activity (100 s, Fig. 3) to record the changes in axial length corresponding to different phases of ipRGC activation; including immediately after, during, and after cessation of the ipRGC stimulation. During the 2-hour defocus period, subjects watched a greyscale movie binocularly at 6 m while remaining seated in a dimly lit room (<10 lux). Under these binocular conditions with +/- 3 D defocus in one eye, the vergence and accommodation cues have been shown to maintain defocus in the intended eye.[36,37] Both defocus conditions were completed within a week for all participants. Two repeats for each stimulus (470 nm and 625 nm) were recorded for each stimulus duration and were averaged for further analysis.

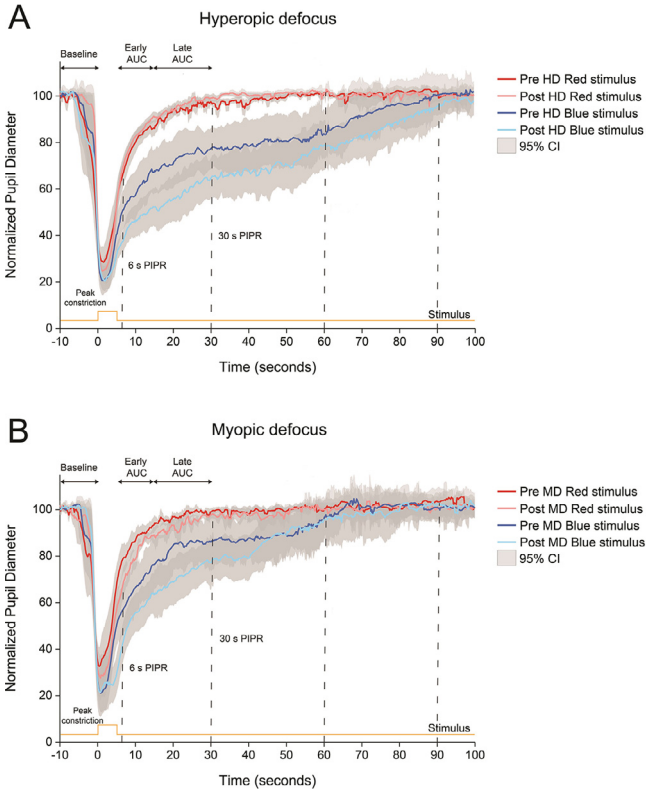

Fig. 3 Normalized pupillary changes for red and blue stimuli before and after 2 h of hyperopic or HD (A) and myopic or MD (B) defocus. Pupil metrics include baseline pupil diameter, peak constriction, 6 s post-illumination pupil response (PIPR), 30 s PIPR, early area under the curve (AUC), late AUC, and time to return to baseline. Shaded regions represent 95% confidence intervals. Stimulus is shown in yellow.

Data analysis

The change in pupil diameter in response to red and blue stimuli was measured from the pupil camera recordings using a custom Matlab program (Matlab 2017b, version 9.3, MathWorks, Natick, MA). For both 1 and 5 s trials, the Matlab program analysed each frame to calculate the change in pupil area relative to the average baseline pupil area for each wavelength (i.e. the average of 10 s pre-stimulus period before red and blue stimulation). The program then generated a time-stamped series of relative pupil responses for further analysis. Data were automatically filtered to remove blinks, and artefacts due to poor fixation during pupil measurements. The PIPR was described by 6 metrics; the peak constriction, the 6 and 30 s PIPR, and the early and late area under the curve (AUC), and time to return to baseline (Table 2).[21,22,25,27,38] All pupil metrics are shown as "normalized change" to the average baseline pupil diameter (expressed in percent). Whilst peak pupil constriction represents both rod/cone and inner retinal activity, the other four metrics are commonly used to describe the ipRGC activity.[21,22]

Two measurements of axial length (i.e. an average of 10 readings) for each subject at each time point were averaged for further analysis. Axial length measurements could not be collected for one participant with myopic defocus. The mean change in axial length with optical defocus was calculated from the difference between the first baseline axial length measurement (prior to 5 s red stimulation), collected before and after 2 h of defocus exposure for all participants. Both pre-and-post-defocus changes in axial length with light stimulation (as shown in Figs. 4 and 5) are normalized to the baseline axial length measurement for individual wavelengths. A sub-analysis of axial length changes was performed on 12 participants that participated in both defocus conditions, and the results were found to be generally

Table 2 Pupil metrics used to quantify photoreceptor contributions to the post-illumination pupil response (PIPR). Metrics include baseline pupil diameter (%), peak constriction (% of baseline), 6 s and 30 s PIPR (% of baseline), early and late area under the curve (AUC, unitless), and time to return to baseline (seconds).

Metric	Definition	Unit	Expected change	Photoreceptor contribution
Baseline pupil diameter	10 s pre-stimulus period before long-and-short-wavelength stimulation	Percent (%)		
Peak constriction	Maximum pupil constriction	% of the average baseline pupil diameter	Smaller value indicates greater constriction	Combination of rod/cone and inner retinal activity
6 s PIPR	Mean pupil diameter 6—7 s after stimulus offset	% of the average baseline pupil diameter	Smaller value indicates greater ipRGC activity	ipRGC activity
30 s PIPR	Mean pupil diameter 30—31 s after stimulus offset	% of the average baseline pupil diameter	Smaller value indicates greater ipRGC activity	ipRGC activity
Early AUC	Log of trapezoidal approximation of the integral of 100% baseline minus the interpolated% pupil diameter, 0—10 s after stimulus offset	Unitless	Larger value indicates greater ipRGC activity	ipRGC activity
Late AUC	Log of trapezoidal approximation of the integral of 100% baseline minus the interpolated% pupil diameter, 10—30 s after stimulus offset	Unitless	Larger value indicates greater ipRGC activity	ipRGC activity
Time to return to baseline	Time taken for the pupil to return to baseline after long-and-short-wavelength stimulation	Seconds	Longer time indicates greater ipRGC activity	Combination of rod/cone and ipRGC activity

similar to the final analysis on 16—17 participants (data not shown). Finally, as all axial length measurements were collected over the contact lens, an assumed lens thickness was later subtracted to account for the additional optical path length (https://coopervision.net.au/).

Statistical analyses were performed using commercial software (SigmaStat 3.5, Aspire Software International, Ashburn, VA). For both hyperopic and myopic defocus, the change in pupil metrics before and after defocus were analysed using two-way ANOVA with "wavelength" and "defocus state" as within-subjects factors. To examine the changes in axial length with red and blue light stimuli for each defocus condition, the two-way repeated-measures ANOVA was used with "time" and "wavelength" as within-subjects factors. To determine the within-subject variability of the PIPR metrics, the intrasession coefficient of variation (CV or SD/mean) was calculated,[22] which has previously been shown to be a reliable measure of variability as it is dimensionless and is not affected by the changes in measurement units.[39] A p-value of less than 0.05 was considered to be statistically significant. All data are expressed as mean ± standard error of mean (SEM).

Results

Effect of ipRGC stimulation on ocular response to hyperopic defocus

Fig. 3 shows the changes in pupil response to red and blue stimuli before and after 2 h of hyperopic and myopic defocus. Compared to the 5 s red stimulus, the blue stimulus induced a strong melanopsin pupillary response both before and after exposure to hyperopic defocus (Fig. 3A). Importantly, the strength of the PIPR with blue light was significantly greater after 2 h of hyperopic defocus, as indicated by significant differences in the 6 s PIPR (pre-defocus, 46.48 ± 3.90%; post-defocus, 38.02 ± 2.29%), 30 s PIPR (pre-defocus, 74.22 ± 4.04%; post-defocus, 57.48 ± 3.67%), early AUC (pre-defocus, 1.37 ± 0.04%; post-defocus, 1.63 ± 0.03%) and late AUC (pre-defocus, 1.31 ± 0.04%; post-defocus, 1.42 ± 0.03%) (two-way ANOVA wavelength by defocus state interaction, all $p<0.05$, Table 3). Exposure to hyperopic defocus attenuated the pupil response to red stimulus as indicated by a decrease of 0.13 units in the late AUC (pre-defocus, 0.82 ± 0.04; post-defocus, 0.69 ± 0.05,

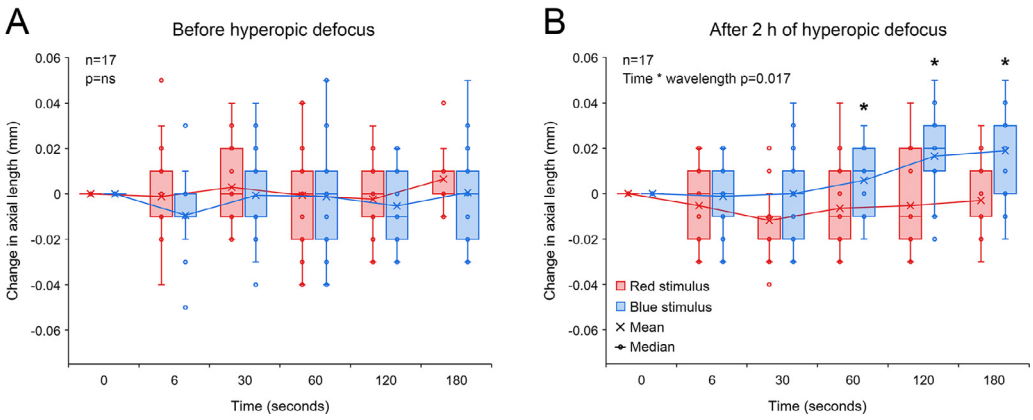

Fig. 4 Change in axial length associated with 5 s red and blue light stimulation before (A) and after 2 h of hyperopic defocus (B). (A) Exposure to red and blue stimuli had no effect on axial length before the introduction of hyperopic defocus (two-way repeated measures ANOVA time by wavelength interaction F(5, 203) = 0.379, p = 0.862). (B) Following 2 h of hyperopic defocus, compared to long-wavelength red stimulus, exposure to short-wavelength blue stimulus resulted in a significant increase in axial length, particularly at 60, 120 and 180 s after stimulus offset (two-way repeated measures ANOVA time by wavelength interaction F(5, 203) = 2.957, p = 0.017). Significant interactions from post-hoc tests are indicated by asterisks.

Holm-Sidak multiple comparisons, $p<0.05$). There were no significant changes in any other pupil metrics with red light stimulation following defocus treatment (Table 3).

2 h of hyperopic defocus resulted in a significant increase in axial length of +0.012 ± 0.006 mm [two-tailed t-test, t (16) = −2.112, p = 0.048]. As shown in Fig. 4A, exposure to red and blue stimuli had no effect on axial length before the introduction of hyperopic defocus (two-way repeated measures ANOVA time by wavelength interaction F(5203) = 0.379, p = 0.862). Following 2 h of hyperopic defocus, melanopsin stimulation with short-wavelength blue light exaggerated the ocular response to defocus, causing a further increase in axial length, which was statistically significant at 60, 120 and 180 s after stimulus offset (two-way repeated measures ANOVA time by wavelength interaction F(5, 203) = 2.957, p = 0.017, Fig. 4B).

Effect of ipRGC stimulation on ocular response to myopic defocus

The 5 s blue stimulus induced a strong PIPR both before and after 2 h of myopic defocus; however, there was no significant interaction between the state of defocus and pupillary changes for either wavelength (two-way ANOVA wavelength by defocus state interaction, all $p>0.05$, Fig. 3B and Table 3).

Two hours of CL induced myopic defocus led to a significant reduction in axial length of −0.014 ± 0.006 mm [two-tailed t-test, t (15) = 2.458, p = 0.037]. However, unlike hyperopic defocus, exposure to 5 s red and blue stimuli had no significant effect on axial length either before or after 2 h of myopic defocus (two-way repeated measures ANOVA time by wavelength interaction, $p>0.05$, Fig. 5).

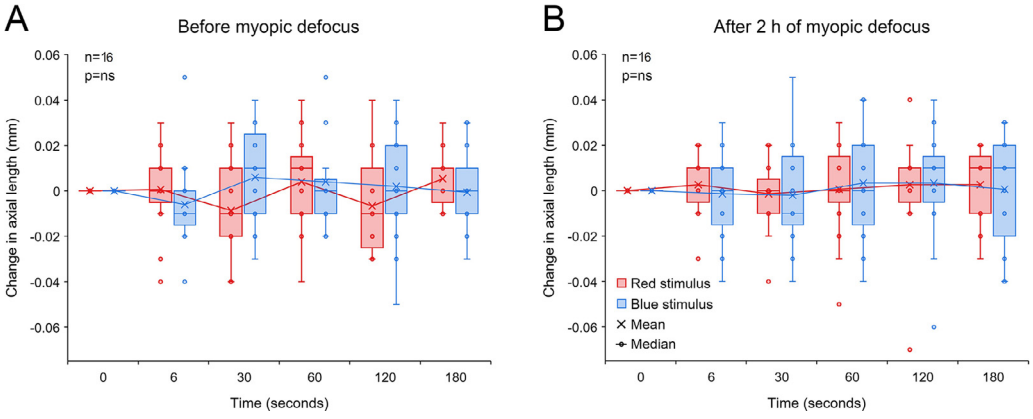

Fig. 5 Change in axial length associated with 5 s red and blue light stimulation before (A) and after 2 h of myopic defocus (B). (A) Exposure to red and blue stimuli had no effect on axial length before the introduction of myopic defocus (two-way repeated measures ANOVA time by wavelength interaction F(5, 179) = 2.102, p = 0.075). (B) Similarly, neither of the two wavelengths had any effect on axial length following 2 h of myopic defocus (two-way repeated measures ANOVA time by wavelength interaction F(5, 179) = 0.267, p = 0.930).

Table 3 Pupil metrics for 5 s red and blue stimuli during axial length measurements before and after 2 h of hyperopic and myopic defocus, along with p-values from two-way ANOVA comparing the main effect of wavelength, defocus state and wavelength by defocus state interaction for each defocus condition. Metrics include baseline pupil diameter (%), peak constriction (% of baseline), 6 s and 30 s post-illumination pupil response (PIPR,% of baseline), early and late area under the curve (AUC, unitless), and time to return to baseline (s). Time to return to baseline was measured until the pupil returned to baseline or end of the ipRGC activity. Significant p values ($p<0.05$) are highlighted in bold.

Defocus	Pupil metrics	Wavelength	Defocus state		p-values		
			Pre-defocus	Post-defocus	Wavelength	Defocus state	Wavelength * defocus state
Hyperopic defocus	Baseline	Red	99.91 ± 0.20%	100.77 ± 0.32%	0.098	0.550	0.219
		Blue	101.28 ± 0.54%	100.98 ± 0.68%			
	Peak constriction	Red	18.91 ± 1.05%	18.95 ± 1.44%	**<0.001**	0.705	0.676
		Blue	12.12 ± 1.07%	11.25 ± 0.59%			
	6 s PIPR	Red	72.20 ± 1.90%	77.25 ± 1.32%	**<0.001**	0.504	**0.010**[¶]
		Blue	46.48 ± 3.90%	38.02 ± 2.29%			
	30 s PIPR	Red	94.58 ± 1.03%	98.65 ± 0.57%	**<0.001**	**0.027**	**<0.001**[¶]
		Blue	74.22 ± 4.04%	57.48 ± 3.67%			
	Early AUC	Red	1.20 ± 0.02	1.16 ± 0.02	**<0.001**	**<0.001**	**<0.001**[¶]
		Blue	1.37 ± 0.04	1.63 ± 0.03			
	Late AUC	Red	0.82 ± 0.04	0.69 ± 0.05	**<0.001**	0.932	**0.007**[¶,#]
		Blue	1.31 ± 0.04	1.42 ± 0.03			
	Time to return to baseline	Red	33.73 ± 2.77	29.54 ± 2.25	**<0.001**	0.582	0.083
		Blue	76.38 ± 4.27	84.41 ± 4.16			
Myopic defocus	Baseline	Red	100.43 ± 0.24%	100.34 ± 0.16%	0.078	0.792	0.936
		Blue	101.36 ± 0.50%	101.19 ± 0.82%			
	Peak constriction	Red	20.68 ± 2.30%	18.12 ± 1.46%	**<0.001**	0.099	0.915
		Blue	14.17 ± 1.53%	11.26 ± 0.91%			
	6 s PIPR	Red	79.79 ± 2.23%	69.05 ± 2.22%	**<0.001**	**0.008**	0.254
		Blue	53.40 ± 3.31%	49.05 ± 3.14%			
	30 s PIPR	Red	99.48 ± 0.74%	96.47 ± 0.92%	**<0.001**	0.121	0.654
		Blue	78.74 ± 2.98%	73.33 ± 4.29%			
	Early AUC	Red	1.09 ± 0.03	1.20 ± 0.03	**<0.001**	0.050	0.890
		Blue	1.32 ± 0.04	1.42 ± 0.09			
	Late AUC	Red	0.62 ± 0.05	0.69 ± 0.03	**<0.001**	0.078	0.577
		Blue	1.16 ± 0.09	1.29 ± 0.05			
	Time to return to baseline	Red	25.20 ± 1.78	32.14 ± 1.99	**<0.001**	0.165	0.659
		Blue	71.69 ± 5.02	75.30 ± 4.90			

[#] Holm-Sidak post-hoc test showed significant differences in the pre-and-post-defocus pupillary changes for the red stimulus ($p<0.05$).
[¶] Holm-Sidak post-hoc test showed significant differences in the pre-and-post-defocus pupillary changes for the blue stimulus ($p<0.05$).

Table 4 Summary of the intrasession coefficient of variation (CV) for each of the PIPR metrics for the myopic and hyperopic defocus experiments (average of pre-and-post defocus). Intrasession CV (expressed in%) was calculated as standard deviation/mean of the two long-wavelength (red) and two short-wavelength (blue) trials. Metrics include baseline pupil diameter, peak constriction, 6 s and 30 s post-illumination pupil response (PIPR), early and late area under the curve (AUC), and time to return to baseline.

Pupil metrics	Intrasession CV (%) for myopic defocus experiment		Intrasession CV (%) for hyperopic defocus experiment	
	Red (625 nm)	Blue (470 nm)	Red (625 nm)	Blue (470 nm)
Baseline	1.11	2.73	1.75	1.87
Peak constriction	11.64	13.67	10.19	12.77
6 s PIPR	5.85	8.27	4.81	7.93
30 s PIPR	6.46	10.01	5.21	9.06
Early AUC	11.75	13.9	11.19	14.48
Late AUC	31.15	33.63	28.82	35.61
Time to return to baseline	16.14	17.84	18.63	18.52

Intrasession variability

To quantify the within-subject variability in the PIPR metrics, we calculated the intrasession coefficient of variation (CV) for each of the pupil metrics (Table 4). The intrasession CV for the peak constriction and the 6 and 30 s PIPR were generally greater for the blue stimulus compared to the red stimulus, but they were all $<$20%, which is considered low and acceptable for PIPR measurements.[22,27] The intrasession CV was significantly greater for AUC parameters and time to return to baseline measurements, particularly for the late AUC with CV $>$20% for both wavelengths (Table 4). The intrasession variability was generally similar between the two defocus conditions (Table 4).

Discussion

In the current study, we found that melanopsin stimulation with blue light exaggerated the ocular response to hyperopic defocus, causing a further increase in axial length above that resulting from the defocus alone. Conversely, melanopsin stimulation had no effect on axial length following myopic defocus. Overall, these findings support a number of recent reports suggesting a possible interaction between melanopsin function and the eye's response to myopiagenic stimuli.[20,40,41]

Similar to our study, a number of previous studies using narrowband short-wavelength blue light (wavelength used across different studies, 448 – 470 nm) and similar irradiance levels to our study have reported a strong PIPR in young healthy subjects.[21-23,25-27,38] We observed a slower pupil redilation after blue stimulation compared to red stimulation independent of the presence or absence, or type of defocus (myopic or hyperopic, Fig. 3). This is indicated by the smaller 6 and 30 s PIPR and larger early and late AUC values, as well as longer time for the pupil to return to baseline following blue light stimulation (Fig. 3 and Table 3).

In our study, the mean change in axial length with hyperopic (+0.012 mm) and myopic defocus (−0.014 mm) were very small. Whist there was no effect of red or blue light stimulation on axial length prior to exposure to defocus, melanopsin stimulation with short-wavelength light following 2 h of hyperopic defocus doubled the ocular response, causing a further increase of approximately +0.018 mm in axial length, particularly at 120 and 180 s after stimulus offset. Although the axial length change with hyperopic defocus represents a small refractive change of $\sim$0.03 D after defocus and 0.05 D after defocus and short-wavelength stimulation, these values were in close agreement with previously reported changes of approximately 10−15 μm in young human eyes in response to short-term optical defocus.[28,29,36,37] These findings suggest a potential interaction between the myopiagenic hyperopic defocus and ipRGC signaling in young subjects. More specifically, we found that melanopsin stimulation exaggerates the ocular response to hyperopic defocus. Whilst a recent study has found that melanopsin signaling plays a key role in protection against form-deprivation myopia in mice through dopaminergic mechanisms,[20] the relationship between melanopsin signaling and ocular growth is more complex. There is a reciprocal interaction between the ipRGCs and DACs, where ipRGCs provide excitatory input to DACs for dopamine release[16,42,43] and in turn, dopamine inhibits the ipRGC function and consequently retinal dopamine release through D1 receptors.[16,44] Furthermore, the synaptic connection between ipRGCs and DACs may not drive global retinal dopamine release.[45,46] Because retinal dopamine is critical in regulating ocular growth and myopia,[18,19] if or how our findings relate to longer-term axial elongation and myopia development warrants further research. Interestingly, melanopsin stimulation had no significant effect on axial length after 2 h of myopic defocus (all axial length changes $<$0.010 mm).

We found that the strength of the PIPR with blue light was significantly greater after 2 h of hyperopic defocus (Fig. 3A), indicating an increased retinal melanopsin activity following sustained exposure to hyperopic defocus. Consequently, it is possible that the increase in axial length with short-wavelength stimulation following hyperopic defocus may be associated with increased melanopsin activity of the retina. These findings suggest that sustained exposure to myopiagenic stimuli (such as minus lens defocus or form-

deprivation) may alter the ipRGC function. Along the same lines, a transcriptome analysis of 6 h of hyperopic defocus with a −15 D lens found altered expression of the melanopsin gene (*Opn4*) in the chick retina, along with altered expression of other intrinsic circadian clock genes, including *Clock* (circadian locomotor out-put cycles kaput), *Cry1* (cryptochrome 1), *Npas2* (neuronalpas domain protein 2), *Per3* (period homolog 3) and *Mtnr1a* (melatonin receptor 1A).[40] Interestingly, these genes were unaffected by myopic defocus with *a* + 15 D lens. Our results combined with the gene studies provide a strong link between hyperopic defocus, melanopsin, and retinal circadian clock signaling.

These findings are interesting because previous studies have found no effect of refractive error on ipRGC-mediated pupil responses in young human subjects.[22,25-27] It is important to note that these studies have all examined the PIPR under 'natural' defocus state (i.e., with the actual uncorrected refractive error). Our study, on the other hand, imposed refractive errors in near emmetropic subjects using defocusing CLs, which mimics the effects of short-term retinal blur experienced during different visual tasks (for e.g., hyperopic defocus experienced during reading or near work). The visual processing of imposed optical defocus can be considerably different from natural defocus in human eyes. For instance, diurnal rhythms of axial length in myopic eyes (experiencing natural myopic defocus) are similar to emmetropic eyes,[47] but exposing the eye to myopic defocus with plus lenses (or imposed myopic defocus) leads to significant changes in the mean amplitude and peak timing of the diurnal rhythms in axial length.[35] Therefore, our results reflect the changes in melanopsin function associated with myopiagenic visual environment (i.e., sustained hyperopic defocus) and not myopic refractive error, as reported previously.

In this study, we used a dark and quiet room for measurements, presented a distant fixation target to induce minimal accommodation, excluded subjects on prescription medication that may affect the pupil size, and performed measurements at a consistent time of the day to avoid any undue influence of accommodation, psychological state, lighting, drugs and autonomic input on pupil measurements.[48] Although autonomic innervation to the pupil cannot be eliminated completely, our measurement protocol ensured that pupillary changes closely represent the ipRGC activity of the eye.

We found that the greatest change in axial length with hyperopic defocus 'plus' blue light stimulation occurred shortly after cessation of the melanopsin activity (i.e. after the pupils had returned to baseline). It took 84 s for the pupil to return to baseline after short-wavelength stimulation following hyperopic defocus; whereas the maximum change in axial length was recorded at 120 and 180 s. This is consistent with intrinsic ipRGC response characteristics of a longer latency and sustained firing during stimulation, and continuous firing following stimulus offset.[12] Nevertheless, as shown in Fig. 4B, the change in axial length with blue stimulation was just noticeable even at 30 s after stimulus offset (although not statistically different from the red stimulus). Based on this, we conjecture that the change in axial length had begun during the melanopsin activation phase (i.e., between 30 and 60 s), but was not captured due to inadequate sampling. It should be noted the strength of melanopsin response, and consequently the magnitude of axial length change may vary with different stimulus irradiance levels, wavelengths and stimulus durations.[21] Future studies looking into the effects of melanopsin stimulation on ocular parameters should consider these factors in their experimental design.

The time lag between melanopsin activation and the greatest axial length changes at 120 and 180 s possibly represents the delay in transduction of visual signals from ipRGCs to other ocular structures, downstream of the retina, that facilitate the changes in axial length. Whilst the present study did not measure changes in any other biometric parameters, it is likely that axial length changes, at least in part, were modulated by changes in choroidal thickness. Previous human studies have reported a significant negative correlation between axial length and choroidal thickness changes with different optical manipulations[29,37] that were evident as early as 5 min after exposure to defocus.[37] Melanopsin phototransduction has been shown to influence choroidal thickness in murine eyes through nonretinal neuronal mechanisms (such as projections to the paraventricular nucleus of the hypothalamus or PVN).[49,50]

In our study, the introduction of CLs could potentially introduce very small errors in axial length measurements. However, the CLs were worn only for a short duration of two hours and any changes in axial length due to CL wear are likely to be very small. We also checked the corneas for all participants at the end of the study and didn't find any significant changes in corneal health. Therefore, any variations in axial length measurements due to CL wear (such as changes in corneal hydration levels) are likely to be small and insignificant. Furthermore, majority of our participants were emmetropic (or near emmetropic) and required the same +3.00 DS (14/16 participants or 88%) and −3.00 DS (14/17 participants or 82%) of CLs. Therefore, any variations related to CL thickness, base curve or other physical parameters between participants were negligible, and would have uniformly influenced all participants in each defocus group.

Similar to previous reports,[21,25] we found that the 625-nm light primarily stimulated the L cones, whereas stimulation with the 470-nm light resulted in excitation of melanopsin cells, rods, and S cones. (Table 1). This happens because all photoreceptors have distinct but overlapping spectral tuning, and even a monochromatic light matched to the peak spectral sensitivity of a given photoreceptor will stimulate other photoreceptors with similar spectral tuning.[51] Therefore, axial length changes with short-wavelength stimulation following hyperopic defocus may be attributed to excitation of melanopsin cells as well as other photoreceptors (rods and S cones). However, based on the relative differences in the individual photoreceptor excitations to red and blue stimuli, we can deduce a significant contribution of melanopsin cells to short-wavelength stimulation. Although beyond the scope of the current research, some studies use the method of silent substitution to specially stimulate the ipRGCs in the living human retina while leaving other classes unstimulated to examine their contribution in the pupillary light response.[51]

Although we reported some significant findings, our study also had limitations. Firstly, it was done on a relatively small sample size consisting of young adults (n = 16−17), so the results may not represent the effects of melanopsin

stimulation on defocus induced axial length changes in other age groups. Secondly, we only recruited near emmetropic subjects with low myopia in the study. Although a previous study found no associations between the ipRGC-driven pupil response and refractive status in children,[26] future studies should examine the effects of melanopsin stimulation on short-term axial length changes in younger populations with high and progressive myopia.

In conclusion, exposure to hyperopic defocus led to a significant increase in the PIPR with blue light. Melanopsin stimulation with blue light exaggerated the ocular response to hyperopic defocus, causing a further increase in axial length than that caused by the defocus alone, which was evident shortly after the cessation of the melanopsin activity. On the contrary, melanopsin stimulation had no effect on axial length associated with myopic defocus. These findings suggest a potential interaction between the myopiagenic hyperopic defocus and the ipRGC system in young human subjects.

Note

Aspects of the article have been presented at the International Myopia Conference (IMC), September 2019 in Tokyo, Japan.

Funding

This work was supported by the Flinders University College of Nursing and Health Sciences Establishment Grant [01.529.41820]; and the Contact Lens and Visual Optics Laboratory, Queensland University of Technology, Brisbane, Australia.

Conflicts of interest

None.

Acknowledgments

We would like to acknowledge Miss Christina Ly, Flinders University, for careful editing of the manuscript.

References

1. Berson DM, Castrucci AM, Provencio I. Morphology and mosaics of melanopsin-expressing retinal ganglion cell types in mice. *J Comp Neurol*. 2010;518:2405–2422.
2. Schmidt TM, Do MT, Dacey D, Lucas R, Hattar S, Matynia A. Melanopsin-positive intrinsically photosensitive retinal ganglion cells: from form to function. *J Neurosci*. 2011;31:16094–16101.
3. Hattar S, Liao HW, Takao M, Berson DM, Yau KW. Melanopsin-containing retinal ganglion cells: architecture, projections, and intrinsic photosensitivity. *Science*. 2002;295:1065–1070.
4. Gamlin PD, McDougal DH, Pokorny J, Smith VC, Yau KW, Dacey DM. Human and macaque pupil responses driven by melanopsin-containing retinal ganglion cells. *Vision Res*. 2007;47:946–954.
5. Berson DM, Dunn FA, Takao M. Phototransduction by retinal ganglion cells that set the circadian clock. *Science*. 2002;295:1070–1073.
6. Sand A, Schmidt TM, Kofuji P. Diverse types of ganglion cell photoreceptors in the mammalian retina. *Prog Retin Eye Res*. 2012;31:287–302.
7. Schmidt TM, Chen SK, Hattar S. Intrinsically photosensitive retinal ganglion cells: many subtypes, diverse functions. *Trends Neurosci*. 2011;34:572–580.
8. Hatori M, Le H, Vollmers C, et al. Inducible ablation of melanopsin-expressing retinal ganglion cells reveals their central role in non-image forming visual responses. *PLoS ONE*. 2008;3:e2451. https://doi.org/10.1371/journal.pone.0002451.
9. Hattar S, Kumar M, Park A, et al. Central projections of melanopsin-expressing retinal ganglion cells in the mouse. *J Comp Neurol*. 2006;497:326–349.
10. Panda S, Sato TK, Castrucci AM, et al. Melanopsin (Opn4) requirement for normal light-induced circadian phase shifting. *Science*. 2002;298:2213–2216.
11. Schmidt TM, Alam NM, Chen S, et al. A role for melanopsin in alpha retinal ganglion cells and contrast detection. *Neuron*. 2014;82:781–788.
12. Dacey DM, Liao HW, Peterson BB, et al. Melanopsin-expressing ganglion cells in primate retina signal colour and irradiance and project to the LGN. *Nature*. 2005;433:749–754.
13. Ecker JL, Dumitrescu ON, Wong KY, et al. Melanopsin-expressing retinal ganglion-cell photoreceptors: cellular diversity and role in pattern vision. *Neuron*. 2010;67:49–60.
14. Schmidt TM, Kofuji P. Structure and function of bistratified intrinsically photosensitive retinal ganglion cells in the mouse. *J Comp Neurol*. 2011;519:1492–1504.
15. Vugler AA, Redgrave P, Semo M, Lawrence J, Greenwood J, Coffey PJ. Dopamine neurones form a discrete plexus with melanopsin cells in normal and degenerating retina. *Exp Neurol*. 2007;205:26–35.
16. Zhang DQ, Wong KY, Sollars PJ, Berson DM, Pickard GE, McMahon DG. Intraretinal signaling by ganglion cell photoreceptors to dopaminergic amacrine neurons. *Proc Natl Acad Sci U S A*. 2008;105:14181–14186.
17. Grunert U, Jusuf PR, Lee SC, Nguyen DT. Bipolar input to melanopsin containing ganglion cells in primate retina. *Vis Neurosci*. 2011;28:39–50.
18. Zhou X, Pardue MT, Iuvone PM, Qu J. Dopamine signaling and myopia development: what are the key challenges. *Prog Retin Eye Res*. 2017;61:60–71.
19. Feldkaemper M, Schaeffel F. An updated view on the role of dopamine in myopia. *Exp Eye Res*. 2013;114:106–119.
20. Chakraborty R, Landis EG, Mazade R, et al. Melanopsin modulates refractive development and myopia. *Exp Eye Res*. 2021;214: 108866. https://doi.org/10.1016/j.exer.2021.108866. Online ahead of print.
21. Adhikari P, Zele AJ, Feigl B. The Post-Illumination Pupil Response (PIPR). *Invest Ophthalmol Vis Sci*. 2015;56:3838–3849.
22. Adhikari P, Pearson CA, Anderson AM, Zele AJ, Feigl B. Effect of age and refractive error on the melanopsin mediated post-illumination pupil response (PIPR). *Sci Rep*. 2015;5:17610.
23. Kankipati L, Girkin CA, Gamlin PD. Post-illumination pupil response in subjects without ocular disease. *Invest Ophthalmol Vis Sci*. 2010;51:2764–2769.
24. Feigl B, Zele AJ. Melanopsin-expressing intrinsically photosensitive retinal ganglion cells in retinal disease. *Optom Vis Sci*. 2014;91:894–903.
25. Abbott KS, Queener HM, Ostrin LA. The ipRGC-Driven Pupil Response with Light Exposure, Refractive Error, and Sleep. *Optom Vis Sci*. 2018;95:323–331.
26. Ostrin LA. The ipRGC-driven pupil response with light exposure in children. *Invest Ophthalmol Vis Sci*. 2017;58:5093.

27. Chakraborty R, Collins MJ, Kricancic H, et al. The intrinsically photosensitive retinal ganglion cell (ipRGC) mediated pupil response in young adult humans with refractive errors. *J Optom*. 2021;S1888-4296(20):30123. https://doi.org/10.1016/j.optom.2020.12.001.
28. Read SA, Collins MJ, Sander BP. Human optical axial length and defocus. *Invest Ophthalmol Vis Sci*. 2010;51:6262—6269.
29. Moderiano D, Do M, Hobbs S, et al. Influence of the time of day on axial length and choroidal thickness changes to hyperopic and myopic defocus in human eyes. *Exp Eye Res*. 2019;182:125—136.
30. Wang D, Chun RKM, Liu M, et al. Optical Defocus Rapidly Changes Choroidal Thickness in Schoolchildren. *PLoS ONE*. 2016;11: e0161535. https://doi.org/10.1371/journal.pone.0161535.
31. Chakraborty R, Read SA, Vincent SJ. Understanding myopia: pathogenesis and mechanisms. editors. In: Ang, Wong, eds. *Updates On Myopia: A Clinical Perspective*. Singapore: Springer Singapore; 2020:65—94.
32. Zele AJ, Feigl B, Smith SS, Markwell EL. The circadian response of intrinsically photosensitive retinal ganglion cells. *PLoS ONE*. 2011;6:e17860. https://doi.org/10.1371/journal.pone.0017860.
33. Ghosh A, Collins MJ, Read SA, Davis BA, Iskander DR. Measurement of ocular aberrations in downward gaze using a modified clinical aberrometer. *Biomed Opt Express*. 2011;2:452—463.
34. Lucas RJ, Peirson SN, Berson DM, et al. Measuring and using light in the melanopsin age. *Trends Neurosci*. 2014;37:1—9.
35. Chakraborty R, Read SA, Collins MJ. Monocular myopic defocus and daily changes in axial length and choroidal thickness of human eyes. *Exp Eye Res*. 2012;103:47—54.
36. Chakraborty R, Read SA, Collins MJ. Hyperopic defocus and diurnal changes in human choroid and axial length. *Optom Vis Sci*. 2013;90:1187—1198.
37. Chiang ST, Phillips JR, Backhouse S. Effect of retinal image defocus on the thickness of the human choroid. *Ophthalmic Physiol Opt*. 2015;35:405—413.
38. Herbst K, Sander B, Milea D, Lund-Andersen H, Kawasaki A. Test-retest repeatability of the pupil light response to blue and red light stimuli in normal human eyes using a novel pupillometer. *Front Neurol*. 2011;2:10. https://doi.org/10.3389/fneur.2011.00010. eCollection 2011.
39. Reed GF, Lynn F, Meade BD. Use of coefficient of variation in assessing variability of quantitative assays. *Clin Diagn Lab Immunol*. 2002;9:1235—1239.
40. Stone RA, McGlinn AM, Baldwin DA, Tobias JW, Iuvone PM, Khurana TS. Image defocus and altered retinal gene expression in chick: clues to the pathogenesis of ametropia. *Invest Ophthalmol Vis Sci*. 2011;52:5765—5777.
41. Stone RA, Khurana TS. Gene profiling in experimental models of eye growth: clues to myopia pathogenesis. *Vision Res*. 2010;50:2322—2333.
42. Zhang DQ, Belenky MA, Sollars PJ, Pickard GE, McMahon DG. Melanopsin mediates retrograde visual signaling in the retina. *PLoS ONE*. 2012;7:e42647. https://doi.org/10.1371/journal.pone.0042647.
43. Atkinson CL, Feng J, Zhang DQ. Functional integrity and modification of retinal dopaminergic neurons in the rd1 mutant mouse: roles of melanopsin and GABA. *J Neurophysiol*. 2013;109:1589—1599.
44. Van Hook MJ, Wong KY, Berson DM. Dopaminergic modulation of ganglion-cell photoreceptors in rat. *Eur J Neurosci*. 2012;35:507—518.
45. Cameron MA, Pozdeyev N, Vugler AA, Cooper H, Iuvone PM, Lucas RJ. Light regulation of retinal dopamine that is independent of melanopsin phototransduction. *Eur J Neurosci*. 2009;29:761—767.
46. Munteanu T, Noronha KJ, Leung AC, Pan S, Lucas JA, Schmidt TM. Light-dependent pathways for dopaminergic amacrine cell development and function. *Elife*. 2018;7:e39866. https://doi.org/10.7554/eLife.39866.
47. Chakraborty R, Read SA, Collins MJ. Diurnal variations in axial length, choroidal thickness, intraocular pressure, and ocular biometrics. *Invest Ophthalmol Vis Sci*. 2011;52:5121—5129.
48. Winn B, Whitaker D, Elliott DB, Phillips NJ. Factors affecting light-adapted pupil size in normal human subjects. *Invest Ophthalmol Vis Sci*. 1994;35:1132—1137.
49. Berkowitz BA, Schmidt T, Podolsky RH, Roberts R. Melanopsin Phototransduction Contributes to Light-Evoked Choroidal Expansion and Rod L-Type Calcium Channel Function In Vivo. *Invest Ophthalmol Vis Sci*. 2016;57:5314—5319.
50. Li C, Fitzgerald ME, LeDoux MS, et al. Projections from the hypothalamic paraventricular nucleus and the nucleus of the solitary tract to prechoroidal neurons in the superior salivatory nucleus: pathways controlling rodent choroidal blood flow. *Brain Res*. 2010;1358:123—139.
51. Spitschan M, Woelders T. The method of silent substitution for examining melanopsin contributions to pupil control. *Front Neurol*. 2018;9:941.